

## Linear and non-linear photo-induced deformations of cantilevers

D. Corbett and M. Warner\*

*Cavendish Laboratory, Madingley Road, Cambridge, CB3 0HE, U.K.*

(Dated: December 11, 2007)

Glassy and elastomeric nematic networks with dye molecules present respond to illumination by reversibly straining because their order parameter is reduced. Elastomers may respond with huge strains and possibly also with director rotation. Appreciable absorption means strain decreases with depth into a cantilever, leading to bend – the basis of micro-opto-mechanical systems (MOMS). Experimentally, bend can occur even when Beer’s law suggests a tiny penetration of light into a heavily dye-doped system. We model general non-linear absorptive processes behind deep penetration into dyes, and also the resultant opto-elastic processes in dye-loaded cantilevers. Bleaching of the active dye species allows deeper penetration of strong beams. When incident light of high intensity gives optimal bending, for a given cantilever thickness, there are three neutral surfaces. We discuss the form of the strains arising when only order parameter reduction is considered. Compressive strains aid director rotation which may be important in elastomeric cantilevers. In practice non-linear absorptive effects are probably important since heavily dye-doped optical cantilevers are commonly used.

PACS numbers:

### I. INTRODUCTION

Nematic elastomers can change their length by large factors on losing or recovering their orientational order. Contraction and elongation respectively arise because the disordering or ordering of rods attached to the nematic network chains causes the chains to become more spherical or elongated, on average. Mechanical strains follow the molecular shape changes of the constituent chains. Nematic order can be decreased or increased by heating or cooling and thus huge thermal strains of up to 500% can be observed [1, 2]. Equally, if rods are also chromophores, that is dye molecules, then absorbing a photon in the straight (*trans*) ground state will cause molecular bend to the (*cis*) excited state and thus disruption of the rod ordering characteristic of the nematic phase. Photo-strains are thus analogous to thermal strains in nematic networks; they are also large and reversible [3, 4]. More densely crosslinked nematic networks suffer small strains on illumination. They have large moduli and are perhaps better called nematic glasses [5]. Unlike elastomers, their directors, the ordering direction on average of rods, seem to be immobile under elongations imposed at an angle and also probably don’t rotate during photo processes [6].

Since photons are absorbed by the dye components in the nematic, then light penetrating the face of a nematic photo-cantilever will be attenuated and hence the contractions generated will diminish with depth. Curvature of the cantilever results, Fig. 1(a). It is important in **micro-opto-mechanical systems** (MOMS) where elements can be optically-induced to bend as elastomeric photo-swimmers [7] or as glassy cantilevers [8, 9]. Sheets of *polydomain* nematic photo-glass can be induced to

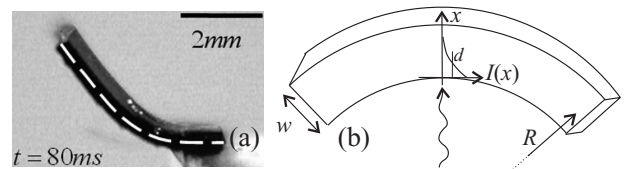


FIG. 1: (a) A cantilever bending towards its side illuminated by a spot (P. Palfy-Muhoray). (b) Radiation penetration with linear absorption length  $d$  giving light-induced bend.

contract by absorption in domains preferentially aligned along the direction of polarisation of light [10]. When there is a significant variation of intensity with depth due to absorption, there is also bend, the direction of which being that of the light polarisation [11]. This important experiment identifies the fundamental effects as optical, rather than thermal effects generated by optical absorption.

Simple absorption, when beams are weak, gives Beer’s law. Intensity exponentially decays with depth and hence there is also an exponentially decaying conversion of straight to bent (*trans*  $\rightarrow$  *cis*) forms of the dye molecules. Assuming a linear connection (valid for small strains) between *cis* population and contraction, one can calculate the cantilever curvature. A maximum curvature is predicted [12] for  $w/d \sim 2.63$ , where  $w$  is the thickness of the cantilever and  $d$  is the exponential decay length: if  $w \gg d$ , only a thin skin of network contracts and its contractile stresses are insufficient to make the unstrained part of the cantilever below respond. Equally, if  $w \ll d$ , then there is little variation of photo-strain through the thickness and the cantilever may contract but not differentially with depth and thus will bend little. The extent of bend, for a fixed  $w/d$ , was also predicted to be linear with intensity.

The purpose of this note is to explain the experimen-

\*Electronic address: mw141@cam.ac.uk

tally common situation where heavily dye-doped cantilevers bend. High dye concentrations mean strong absorption and hence small  $d$ . Thus one is frequently in the thin-skin limit  $d \ll w$ , where bend might be expected to disappear, and yet appreciable mechanical effects are still seen [13]. We shall explain this effect for the more straight forward case of no photo-induced director rotation, that is for nematic glasses, or for elastomers with diffuse illumination. Director rotation has been explored in polydomain photo-elastomers and may be complex [10]. The remainder of this paper is organised as follows. In section II we derive equations which describe the attenuation of light passing through a region with photo-active chromophores. Our analysis of non-linear absorption is thus relevant to a wide range of situations where dye is irradiated, and is not limited to mechanics, which is our ultimate aim here. In section III we show how attenuation leads to cantilever bending and calculate the radius of curvature as a function of the incident flux of light. In section IV we investigate the distribution of strain throughout the bent sample, and in particular we demonstrate that there can be several planes throughout the cantilever on which the net strain is zero. In section V we discuss the possible effects of temperature change owing to absorption of photons on the results presented thus far. Our analysis suggests that for intense illumination temperature distributions are symmetric about the cantilever mid-plane and hence do not contribute to bend, only contraction. Finally in VI we present our conclusions.

## II. ATTENUATION

We consider the situation of Fig. 1(b) of a long, slender cantilever of thickness  $w$  illuminated by light with incident flux  $I_0$ . The absolute number density of chromophores is  $\rho_{ph}$ . At a time  $t$  after the onset of illumination and depth  $x$  within the cantilever, the fraction of these chromophores in the straight *trans* state is  $n_t(x, t)$  and the fraction in the bent *cis* state is  $n_c(x, t) = 1 - n_t(x, t)$ . The magnitude of the Poynting flux at  $x$  and  $t$  is  $I(x, t)$ . The dynamics of the *trans* fraction is determined by three processes, (i) an optically stimulated *trans*  $\rightarrow$  *cis* reaction with rate  $\Gamma_1 I(x, t) n_t(x, t)$ , (ii) an optically stimulated *cis*  $\rightarrow$  *trans* back-reaction with rate  $\Gamma_2 I(x, t) n_c(x, t)$  and (iii) a spontaneous, thermally activated, *cis*  $\rightarrow$  *trans* back-reaction with characteristic time  $\tau$ .  $\Gamma_t$  and  $\Gamma_c$  subsume absorption cross sections per chromophore and the quantum efficiencies  $\Phi_{tc}$  and  $\Phi_{ct}$  of the stimulated *trans-cis* reaction and *cis-trans* back-reaction respectively, see [14] for the rate equations in full with such factors explicitly given. We take the absorption cross sections to be independent of nematic order – itself another source of non-linearity that is discussed in the polydomain elastomer case [10]. Combining these three rates we obtain for the

rate of change of the *trans* fraction:

$$\frac{\partial n_t}{\partial t} = -\Gamma_t I(x, t) n_t(x, t) + \left( \frac{1}{\tau} + \Gamma_c I(x, t) \right) n_c(x, t) \quad (1)$$

In this paper we confine ourselves to the steady-state, that is  $\frac{\partial n_t}{\partial t} = 0$ . Setting this condition in eqn (1) and taking out a factor of  $\tau$  gives the steady state *trans* and *cis* populations:

$$n_t(x) = \frac{1 + \Gamma_c \tau I}{1 + (\Gamma_t + \Gamma_c) \tau I} ; n_c(x) = \frac{\Gamma_t \tau I}{1 + (\Gamma_t + \Gamma_c) \tau I} \quad (2)$$

where  $I$  is now  $I(x)$  simply, and will be determined below. We can identify two characteristic, material intensities,  $I_t = 1/(\Gamma_t \tau)$  and  $I_c = 1/(\Gamma_c \tau)$ . It is convenient to scale the flux by its incident value, thus  $\mathcal{I}(x, t) = I(x, t)/I_0$ . The reduced intensity is thus  $\mathcal{I} = 1$  at the entry surface  $x = 0$ , see Fig. 1(b). We also define dimensionless quantities  $\alpha = I_0/I_t$  and  $\beta = I_0/I_c$ . Ignoring for the moment attenuation,  $\alpha$  measures how much a beam intensity  $I_0$  leads to *trans* conversion, eqn (1), by comparing  $I_0$  to  $I_t$ , that is the ratio of the forward rate to the thermal backward rate,  $\alpha = I_0/I_c = I_0 \Gamma_t / (1/\tau)$ . Likewise,  $\beta$  is the ratio of the induced to the thermal back rates.

In terms of the reduced incident intensities  $\alpha$  and  $\beta$ , the steady state *trans* and *cis* populations are given by:

$$n_t(x) = \frac{1 + \beta \mathcal{I}}{1 + (\alpha + \beta) \mathcal{I}} ; n_c(x) = \frac{\alpha \mathcal{I}}{1 + (\alpha + \beta) \mathcal{I}} \quad (3)$$

Here  $\mathcal{I}$  is just  $\mathcal{I}(x)$  since we have the equilibrium case. In the Eisenbach experiments [15] the average conversion was  $n_c \sim 0.84$ . His measurements of attenuation suggested  $\beta \sim 0$ , and thus one can conclude from eqn (3) that his  $\alpha \sim 5$ . Note that  $\alpha$  and  $\beta$  are independent of chromophore concentration, but do depend on the choice of the light polarisation [14]. Experimentally it is easiest to determine  $\alpha$  for a system dilute in chromophores, where one can ignore the complications arising when attenuation is significant. These estimates for  $\alpha$  are lower bounds on actual values; including the effects of attenuation through the cantilever will lead to higher values of  $\alpha$ . In later work [3] one can deduce that  $\alpha \sim 0.8$ .

The divergence of the Poynting flux,  $\frac{\partial I}{\partial x}$ , at any point through the cantilever is equal to the amount of energy taken out of the beam per unit volume per unit time. For simplicity, we ignore curvature leading to obliquity factors for the intensity of light falling on the surface. That is, we consider small deflections or diffuse light. Energy is taken out of the beam both by the optically induced *trans*  $\rightarrow$  *cis* reaction and by the stimulated *cis*  $\rightarrow$  *trans* back-reaction, terms (i) and (ii) above. The divergence of the Poynting flux is thus related to the sum of the rates of these two processes. Thus:

$$\frac{\partial I}{\partial x} = -\gamma_t \Gamma_t I(x, t) n_t(x, t) - \gamma_c \Gamma_c I(x, t) n_c(x, t) \quad (4)$$

where the constant  $\gamma$  in each case subsumes the energy of an incident photon,  $\hbar\omega$ , the absolute number density of chromophores,  $\rho_{ph}$ , and the reciprocal of the quantum

efficiency  $\Phi$  for the relevant transition. The appearance of  $\Phi$  as an inverse is required since for each successful transition in the rate  $\Gamma_i I n_i$  ( $i = t, c$ ) there will be unsuccessful absorptions that do not contribute to  $\partial n_t / \partial t$  in (1), but nevertheless still deplete the optical beam and contribute to  $\partial I / \partial x$  in (4).

Eqns (1) and (4) are a pair of coupled, non-linear, first order partial differential equations for  $I(x, t)$  and  $n_t(x, t)$ . Solving these equations subject to the boundary conditions  $I(0, t) = I_0$  and  $n_t(x, 0) = 1$  is in general complex, though analytically possible in some limits. We return to this problem elsewhere and here take the equilibrium state. Thus, using  $n_c = 1 - n_t$ , dividing through by the incident intensity  $I_0$ , and letting  $d_t = 1/(\gamma_t \Gamma_t)$  and  $d_c = 1/(\gamma_c \Gamma_c)$  denote the characteristic lengths for optical attenuation by *trans* and *cis* chromophores respectively, one obtains [14, 16]

$$\frac{d\mathcal{I}}{dx} = - \left( \left[ \frac{1}{d_t} - \frac{1}{d_c} \right] n_t + \frac{1}{d_c} \right) \mathcal{I}(x). \quad (5)$$

Note that the derivative has become a full derivative, since time is no longer a relevant variable. In terms of the parameters  $\alpha$  and  $\beta$ , the ratio of the *trans* and *cis* lengths is  $d_t/d_c = (\gamma_c/\gamma_t)(\beta/\alpha)$ . The ratio  $\eta = \gamma_c/\gamma_t$  is the ratio of the quantum efficiencies for the *trans*  $\rightarrow$  *cis* and *cis*  $\rightarrow$  *trans* reactions, that is  $\eta = \Phi_{tc}/\Phi_{ct}$ . We shall take  $\eta = 1$  in the numerical illustrations in this paper. We have ignored any attenuation by the background material; one could include such effects by adding a simple Lambert-Beer term  $-I(x, t)/d_{bg}$  to the RHS of eqn (4). Such absorption turns out to renormalize the intensity but otherwise not change our results qualitatively.

Inserting the steady-state expression for  $n_t$  from eqn (3) into eqn (5), and then integrating w.r.t.  $x$ , subject to  $\mathcal{I}(x=0) = 1$ , we obtain:

$$\ln \mathcal{I} + \left( \frac{\alpha - \beta' + \beta}{\beta'} \right) \ln \left( \frac{1 + \beta' \mathcal{I}}{1 + \beta'} \right) = -\frac{x}{d_t}, \quad (6)$$

where  $\beta' = \beta(1+\eta)$ . In general this expression is very different from Beer's Law,  $\mathcal{I}(x) = \exp(-x/d)$ , but reduces to this form in various limits.

The deviation from Beer's Law comes about because at high intensities the *cis* population increases (bleaching) and is generally less absorbing than the *trans* species. Optical penetration is then more effective and is of great significance for photo-mechanics. To see how non-linearities (bleaching) manifest themselves, consider the limit  $\beta \rightarrow 0$  [16] that arises when stimulated *cis* back-conversion is weak (for instance in the work of Eisenbach). Under those circumstances  $\Gamma_c \sim 0$  in eqn (1), and then (5) takes the form:

$$\frac{d\mathcal{I}}{dx} = -\frac{n_t}{d_t} \mathcal{I}(x). \quad (7)$$

A non-Beer form arises because  $n_t = 1/(1 + \alpha \mathcal{I})$  itself depends on  $\mathcal{I}$ , eqn (3). Integration gives

$$\ln \mathcal{I} + \alpha(\mathcal{I} - 1) = -x/d_t, \quad (8)$$

also a  $\beta \rightarrow 0$  limit of (6). A formal solution of which is  $\mathcal{I}(x) = W_L(\alpha e^{-x/d_t})/\alpha$ , where  $W_L(x)$  is the Lambert-W function [17]. The non-exponential decay persists until around  $\alpha \mathcal{I} < 1$ , whereupon  $n_t$  becomes independent of  $\mathcal{I}$  and (7) reverts to simple exponential form. We illuminate this non-linear absorption more fully below, e.g. in Fig. 2.

The limiting cases of absorption are important.

(i)  $(\alpha + \beta)\mathcal{I} \ll 1$ . Now  $n_t \approx 1$  and  $n_c \approx 0$  which renders (5) trivially of the Beer form. The limit obtains when  $\alpha = I_0/I_t$  and  $\beta = I_0/I_c$  are both  $\ll 1$  (since  $\mathcal{I}$  is bounded by 1), that is, the incident beam is weak compared with the material fluxes  $I_t$  and  $I_c$ . It also obtains when  $\alpha$  and  $\beta$  are not small, but when  $\mathcal{I} \ll 1/(\alpha + \beta)$ , that is when the beam has diminished (albeit linearly rather than exponentially, see Fig. 2) to the point that  $n_t \approx \text{const.}$  and Beer behavior is finally recovered. From (8) one sees in fact  $\mathcal{I}(x) \sim \exp[-(x - d_t \alpha)/d_t]$  for  $x > d_t \alpha$ , a shifted Beer form. This is the ultimate fate of all optical beams provided that cantilevers are thick enough to get this diminution of intensity.

(ii) The high flux limit,  $\beta \mathcal{I} \gg 1$ , that is  $I \Gamma_c \gg 1/\tau$ , is where the stimulated back-reaction dominates over the thermal back-reaction. In that case  $n_t \rightarrow \beta/(\alpha + \beta)$  and  $n_c \rightarrow \alpha/(\alpha + \beta)$  are again constants and again (4) takes a Beer form in the equilibrium limit:

$$d\mathcal{I}/dx = -\mathcal{I}\beta(1 + \eta)/(d_t(\alpha + \beta)). \quad (9)$$

The decay is exponential,  $\mathcal{I} = \exp(-x/d_{\text{eff}})$  with an effective decay length  $d_{\text{eff}} = d_t(\alpha + \beta)/(\beta(1 + \eta))$ .

Thus, except for  $\beta = 0$ , profiles start in a Beer-manner, have an intermediate non-exponential behavior if we have  $\alpha > 1$  with  $\beta \ll \alpha$ , and then conclude with another Beer decay. The intermediate regime,  $\beta \mathcal{I} \sim 1$ , is where the stimulated back reaction rate is comparable to the thermal rate.

(iii) When the decay lengths accidentally coincide,  $d_t = d_c$ , that is  $\gamma_t \Gamma_t = \gamma_c \Gamma_c$ , one can easily see in either (4) or in (5) that a Beer form pertains at all intensities or depths into the photoisomerising medium:  $\mathcal{I} = \exp(-x/d_c)$ .

Statman and Janossy [14] investigated photoisomerisation of solutions of the commercially available azodye Disperse Orange (DO3). They obtained a ratio of  $\alpha/\beta \sim 5$  while the accessible range of  $\alpha$  is up-to  $\sim 80$  (corresponding to an incident flux of 15mW/mm<sup>2</sup>). The spectral bands for *trans*  $\rightarrow$  *cis* and *cis*  $\rightarrow$  *trans* overlap quite strongly for DO3; one might thus expect much smaller ratios of  $\beta/\alpha$  to be accessible when using dyes with more separated absorption bands. Indeed, Eisenbach's attenuation study showed that, for his systems,  $d_c \gg d_t$  and thus that  $\alpha \gg \beta$ , possibly  $\alpha \sim 100 \times \beta$ . We thus show results initially for very high ratios  $\alpha/\beta$  for a range of incident intensities  $\alpha$  and then look at smaller ratios where the non-linear region is not so pronounced.

As can be seen from eqn (3), the *cis* population is always reduced when  $\beta$  is finite. Thus for non-zero  $\beta$  we require a larger value of  $\alpha$  to achieve a particular value of  $n_c$ . Similarly attenuation will lead to reduced intensities lower than unity in eqn (3), again requiring larger

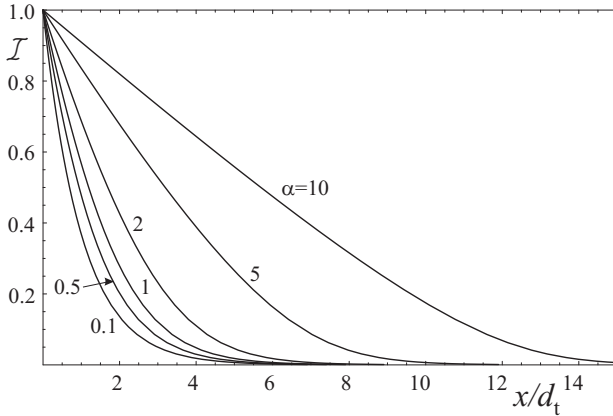


FIG. 2: The decay in reduced light intensity with reduced depth for various reduced incident intensities  $\alpha = I_0/I_c$ . Photo-induced back-reaction is minimal,  $\beta = 0$ .

values of  $\alpha$  to achieve the same *cis* concentration. Thus estimates of  $\alpha$  from absorption are lower bounds on true values.

#### A. CASE 1 - $\alpha/\beta = \infty$

We start with the case in which the illuminating light doesn't excite the *cis*  $\rightarrow$  *trans* back-reaction at all, i.e.  $\beta = 0$ . Thus the intensity is described by eqn (8). Fig. 2 shows how for low  $\alpha$  the decay from the surface intensity is exponential, but that penetration is much deeper for higher  $\alpha$ , being initially a linear decay until finally decaying as an off-set exponential beyond the characteristic depth  $d_t$ , that is for  $x > d_t\alpha$ .

Such non-exponential behavior suggests caution when trying to establish an extinction length from the attenuation of a light beam on traversing a cantilever. For instance [13] an attenuation of 99% on traversing a cantilever of thickness  $1\mu\text{m}$ , were Beer's Law being followed, would result from an extinction length of  $d_{\text{Beer}} = 1\mu\text{m}/(2\ln(10)) \sim 0.22\mu\text{m}$ . But if  $\alpha$  is not small, much more light penetrates to  $x = w$  (Fig. 2). The  $d_{\text{Beer}}$  value derived is a gross over-estimate of  $d_t$ . Solving for  $d_t$  from eqn (8) for a given attenuation  $\mathcal{I}(w)$  on reaching the back face at  $x = w$  yields for 99% attenuation:  $d \sim w/(\alpha + 4.6) = 1\mu\text{m}/(\alpha + 4.6) \rightarrow 0.04\mu\text{m}$  for  $\alpha = 20$ . The true  $d_t$  associated with a possible exponential decay may thus be much lower than the value  $d_{\text{Beer}}$  estimated as above, an indication that light has penetrated much further into the sample than would be expected for a simple exponential profile. Quantitative measurements of light attenuation varying with thickness or varying with incident intensity would resolve this ambiguity about  $d_t$  and also allow a determination of  $\alpha$ . Attenuation at one thickness can only give an upper bound on  $d_t$ .

The reasons for departures from Beer's law for the intensity can be seen by returning the solution  $\mathcal{I}(x)$  to eqn (3) for the *cis* concentration. Fig. 3 displays ex-

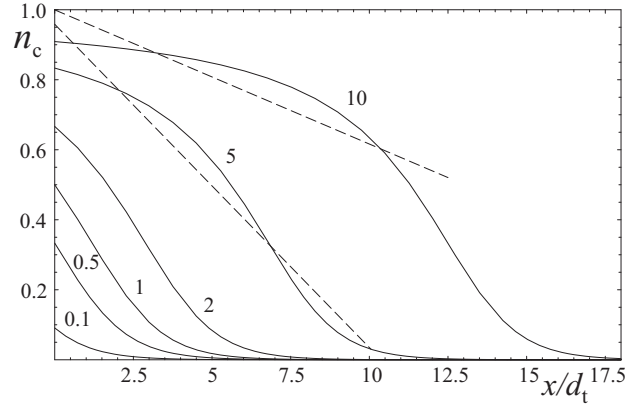


FIG. 3: Number fraction  $n_c(x)$  of dye molecules converted to *cis* against reduced depth  $x/d$  for various reduced incident light intensities,  $\alpha$ . Photo-induced back-reaction is minimal,  $\beta = 0$ . Increasing  $\alpha$  extends the conversion to greater depths because of photobleaching of the surface layers. Reduced geometric bend strain for  $\alpha = 5, 10$  are shown as straight dotted lines. For cantilevers of thickness  $w = w^* = 10.053d$  and  $w = 12.5d$  respectively, there are three and two intersections (neutral surfaces) with the photo-strain curves.

ponential decay in  $n_c$  following  $\mathcal{I}(x)$  for low intensity ( $\alpha = 0.1, 0.5$ ). High incident intensity not only lifts  $n_c(x = 0)$  at the surface, but also flattens the decay with depth – high  $n_c$  means low  $n_t = 1 - n_c$  and hence fewer *trans* dye molecules in a state to deplete the incoming beam (a photo-bleached state). With photo-bleached surface layers, radiation penetrates well beyond  $x \sim d_t$ , and equally, contraction extends deep into the bulk, certainly beyond the Beer penetration depth  $d_t$ .

For  $\alpha = 0.5$  a point of inflection first appears at the surface, and moves inwards with increasing incident intensity  $\alpha$ . The *cis* fraction at the inflection is always  $n_c = 1/3$  in this model. In the general case where  $\beta \neq 0$  we find that the value of  $\alpha$  at which the point of inflection first appears at the front surface is a complicated function of the constant ratio  $\beta/\alpha$ , and the value of the *cis* fraction at the inflection point is no longer  $1/3$ . From eqn (3), the surface *cis* concentration is  $n_c(0) = \alpha/(1+\alpha)$ , since there  $\mathcal{I} = 1$ , and rises to saturation,  $n_c = 1$ , as intensity increases. The precise form of the cantilever bend depends critically on the shape of these  $n_c(x)$  curves. In particular the development of a point of inflection allows three intercepts of the straight, geometric strain curves, and thus three neutral surfaces, we will later see. Since  $n_c(x)$  changes shape with increasing intensity, we will find an elastic response that is highly non-linear with intensity.

#### B. CASE 2 - $\alpha/\beta = 50$

We now consider the case with a weakly stimulated back-reaction,  $\beta = \alpha/50$ , and henceforth take  $\eta = 1$ . Fig 4 shows plots of the reduced intensity as a function of  $x/d_t$  for equivalent values of  $\alpha$  chosen in Fig 2.

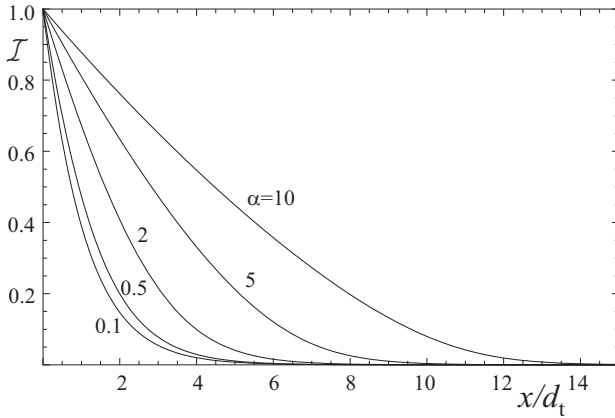


FIG. 4: The decay in reduced light intensity with reduced depth for various reduced incident intensities  $\alpha$ , with a weakly stimulated back reaction such that  $\alpha/\beta = 50$ . The plots are similar to those shown in figure 2.

The reduced intensity curves are largely identical to those shown in Fig 2. Once again, for small values of  $\alpha$  ( $=0.1, 0.5$ ) the decay is essentially exponential, with a characteristic length given by  $d_t$ . Increasing  $\alpha$  leads to deeper penetration, with the initial decay being essentially linear. However close inspection of the  $\alpha = 10$  curve reveals a slight upwards curvature, a result of the higher order corrections in  $\beta$  that take us from (8) to (6). Eventually  $\mathcal{I}(x)$  becomes exponential at penetration depths  $x \sim d_t \alpha$  significantly greater than  $d_t$ .

As we show above, for  $\beta \gtrsim 1$ , that is here  $\alpha \gtrsim 50$ , the initial behaviour should revert to being exponential before attaining the linear decay associated with non-Beer. This point is easier to display below when we consider smaller  $\alpha/\beta$  ratios.

The *cis* profiles as a function of depth are shown in Fig 5 and should be compared with those in Fig 3. For the values of  $\alpha$  plotted, the curves are essentially identical. High incident intensities result in larger *cis* fractions near the surface, and a flatter decay as before. The point of inflection occurs for a *cis* fraction less than the  $1/3$  found in the  $\beta = 0$  case, but it is of equal importance that inflections exist for the mechanics we explore later.

### C. CASE 3 - $\alpha/\beta = 5$

Increasing the stimulated back reaction further we take  $\alpha/\beta = 5$ . The curves for the reduced intensity as a function of depth, see Fig 6, now differ somewhat from those in Fig 2. For the smaller values of  $\alpha$  the curves remain exponential with a characteristic length  $d_t$ . Increasing  $\alpha$  leads to some increased penetration, without showing the long linear decay in reduced intensity seen in Figs 2 and 4. For  $\alpha = 10$  we have  $\beta\mathcal{I} = 2$  at most, a value evidently insufficient to satisfy limit (ii). We do not have a finite initial region for small  $x$  where the decay is exponential

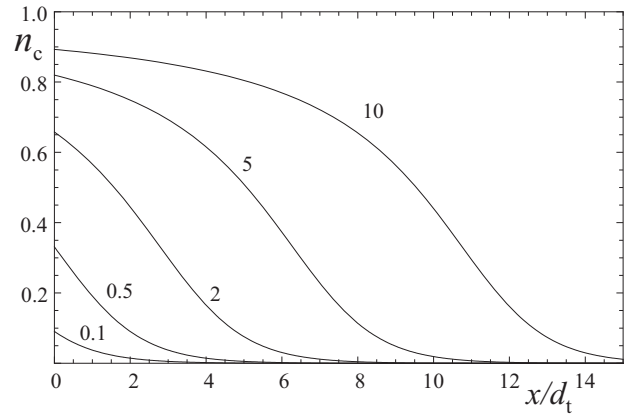


FIG. 5: The decay in *cis* number fraction  $n_c(x)$  with reduced depth for various reduced incident intensities  $\alpha$ , with  $\alpha/\beta = 50$ .

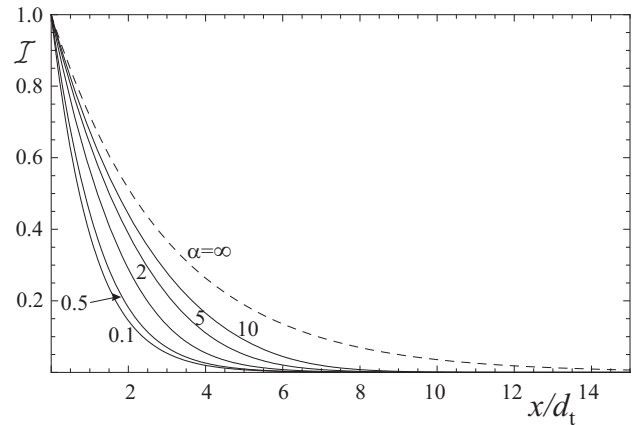


FIG. 6: The decay in reduced light intensity with reduced depth for various reduced incident intensities  $\alpha$  with  $\alpha/\beta = 5$ .

with  $d_{\text{eff}}$  given in and below eqn (9). For these values of  $\alpha$  and  $\beta$  one would have  $d_{\text{eff}} = 3d_t$ . The dashed line shows the infinite  $\alpha$  limit, and corresponds throughout its range to eqn (9), i.e. an exponential with characteristic length  $d_{\text{eff}} = d_t(\alpha + \beta)/(\beta(1 + \eta)) = 3d_t$ . Note that the initial of the  $\alpha = 10$  curve is close to that of the  $\alpha = \infty$  curve.

### III. OPTICALLY-INDUCED CURVATURE

Fig. 1(b) shows a cantilever with radius of curvature  $R$ . The geometric strain from bending is  $x/R + K$ , where  $R$  is the radius of curvature adopted by the cantilever and  $K$  is a mean contraction, both to be determined for a given thickness  $w$  and illumination. Illumination changes the natural length of the sample, the actual strain with respect to this new natural length is  $x/R + K - \epsilon_p$  which, if we further reduce  $x/R$  and  $K$  by the dimensionless constant  $-A$  connecting photo-strain  $\epsilon_p$  and the *cis* concentration, we obtain  $x/R + K + n_c(x)$  for the effective reduced strain. The mechanical stress  $\sigma$  is related linearly to the strain via the Young's modulus  $E$ .

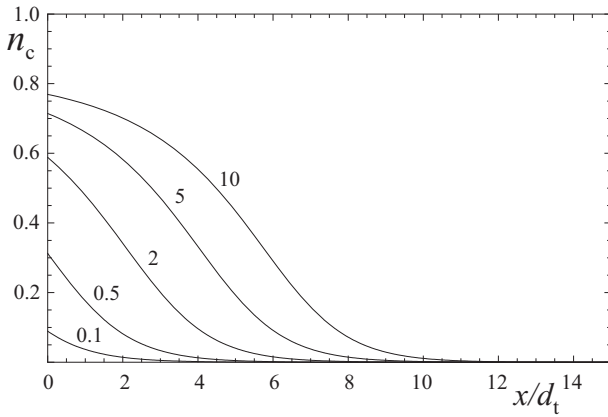


FIG. 7: The decay in *cis* number fraction  $n_c(x)$  with reduced depth for various reduced incident intensities  $\alpha$  with  $\alpha/\beta = 5$ .

Since there are no external forces nor external torques, mechanical equilibrium requires vanishing total force and moment across a section, thus:

$$\begin{aligned} \int_0^w \sigma(x) dx &= E \int_0^w \left( \frac{x}{R} + K + n_c(x) \right) dx = 0, \\ \int_0^w x \sigma(x) dx &= E \int_0^w x \left( \frac{x}{R} + K + n_c(x) \right) dx = 0. \end{aligned} \quad (10)$$

When the modulus is constant it drops out, but must generally be retained (for some photo-glasses  $E$  is known to vary with illumination [6]). Performing these integrations we have:

$$\frac{w^2}{2R} + Kw = - \int_0^w n_c(x) dx \quad (11)$$

$$\frac{w^3}{3R} + \frac{Kw^2}{2} = - \int_0^w xn_c(x) dx. \quad (12)$$

Simplifying between these two expressions we obtain for the radius of curvature:

$$\frac{1}{R} = \frac{12}{w^3} \int_0^w \left( \frac{w}{2} - x \right) n_c(x) dx \quad (13)$$

Eqn (5) can be rearranged to give an expression for  $n_c(x)$ , recalling  $d_t/d_c = \eta\beta/\alpha$ ,  $\eta = \gamma_c/\gamma_t$ , and  $n_t = 1 - n_c$ :

$$n_c(x) = \frac{1}{1 - \eta \left( \frac{\beta}{\alpha} \right)} + \frac{d_t}{1 - \eta \left( \frac{\beta}{\alpha} \right)} \frac{1}{\mathcal{I}} \frac{\partial \mathcal{I}}{\partial x}, \quad (14)$$

Inserting this expression into eqn (13) and changing integration variables  $\int_0^w dx \rightarrow \int_{\mathcal{I}_0=1}^{\mathcal{I}_w} d\mathcal{I}$  we have:

$$\frac{d_t}{R} = 12 \left( \frac{d_t}{w} \right)^3 \frac{1}{1 - \eta \left( \frac{\beta}{\alpha} \right)} \int_1^{\mathcal{I}_w} \left( \frac{w}{2d_t} - \frac{x}{d_t} \right) \frac{d\mathcal{I}}{\mathcal{I}}. \quad (15)$$

Substituting for  $x/d_t$  and  $w/d_t$  from eqn (6) and performing the integration, we ultimately obtain (with  $\beta' =$

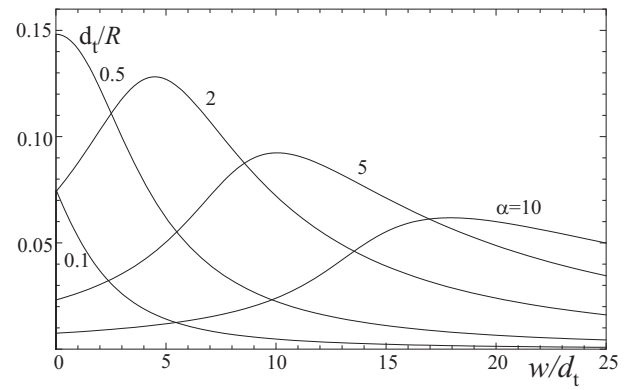


FIG. 8: Curvature reduced by  $1/d_t$  against reduced cantilever thickness  $w/d_t$  for various incident reduced light intensities  $\alpha$  (with  $\beta = 0$ ). For high intensities, bleached surface layers let light penetrate more deeply and hence a significant fraction of the cantilever has its natural length contracted. Bend occurs even for cantilevers much thicker than the linear penetration depth  $d_t$ .

$\beta(1 + \eta)$ :

$$\frac{d_t}{R} = \frac{12\alpha}{\beta' (w/d_t)^3} \left[ Li_2(-\beta') - Li_2(-\beta' \mathcal{I}_w) - \frac{1}{2} \ln(\mathcal{I}_w) \ln[(1 + \beta' \mathcal{I}_w)(1 + \beta')] \right] \quad (16)$$

where  $Li_2(x) = \int_x^0 dt \frac{\ln(1-t)}{t} = \sum_{k=1}^{\infty} \frac{x^k}{k^2}$  is the dilogarithm [18]. The limit  $\beta \rightarrow 0$  within this expression recovers our earlier expression for the curvature [16]:

$$\begin{aligned} \frac{d_t}{R} &= \frac{12\alpha d_t^3}{w^3} \times \\ &\times \left[ \frac{w}{d_t} \mathcal{I}_w - (1 - \mathcal{I}_w) \left( 1 - \frac{w}{2d_t} \right) - \frac{\alpha}{2} (1 - \mathcal{I}_w^2) \right] \end{aligned} \quad (17)$$

At low incident light intensity,  $\alpha \rightarrow 0$ , analysis [12] for exponential decay gave maximal reduced curvature  $w/\alpha R$  for  $w/d \sim 2.63$ . In this limit  $1/R \sim \alpha \sim I_0$ , hence the division by  $\alpha$  to obtain results universal for all (low) intensities of incident light. As intensity increases, the maximum in  $w/\alpha R$  moves to larger  $w/d$  because the radiation penetrates more deeply.

The non-linear regime, at fixed Beer's Law penetration  $d_t$ , is best revealed by reducing  $R$  by  $d_t$  instead of by  $w$ , and by not reducing  $1/R$  by  $\alpha$ . Fig. 8 plots  $d_t/R$  against  $w/d_t$  to reveal maxima in  $d/R$  at greater  $w$  as intensity  $\alpha$  and thus penetration increases. At a given  $w/d_t$ , one sees curvature increase initially with intensity, the Beer limit, and then reduce as penetration increases and gradients of strain are reduced. Thus appreciable curvature arises experimentally even in cantilevers thick in the sense  $w \gg d_t$ : in [11] it appears that curvature is induced even though the cantilevers involved (with  $w = 10 \mu\text{m}$ ) are apparently at least 100 times thicker than their extinction length! (See also [13].) The curvatures against thickness for various intensities  $\alpha$  in the case of

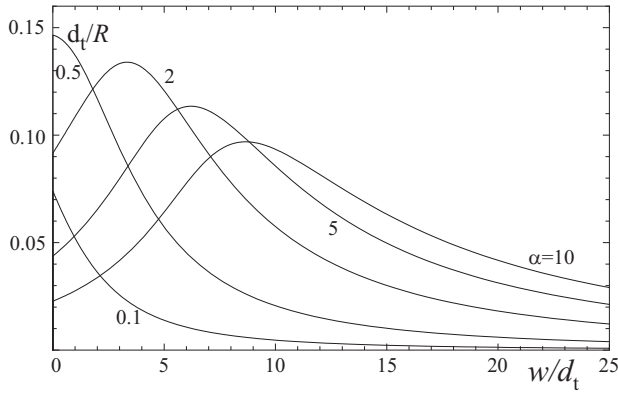


FIG. 9: Curvature reduced by  $1/d_t$  against reduced cantilever thickness  $w/d_t$  for various incident reduced light intensities  $\alpha$  (with  $\alpha/\beta = 5$ ). Maxima in curvature occur at smaller thicknesses than in the  $\beta = 0$  case where back reaction is purely thermal.

$\alpha/\beta = 50$  studied above are practically identical to those in the  $\beta = 0$  limit of Fig. 8. As the back-reaction rate increases relative to the forward rate,  $\alpha/\beta = 5$ , the penetration is less and the curvature maxima move to noticeably smaller reduced thicknesses  $w/d_t$ , see Fig 9. Quantitative measurements of reduced curvature  $w/R$  with  $I_o$  are required to probe this complex dependence of curvature on thickness and incident intensity.

#### IV. STRAIN DISTRIBUTIONS

In the linear case [12] of bend induced by exponentially decaying optical intensity, two neutral surfaces arise, that is surfaces of zero stress where the geometric strains arising from curvature happen to match the local photo-strain:  $x_n/R + K + n_c(x_n) = 0$ . A classical cantilever bent by imposed terminal torques has a single neutral surface at its mid-point  $x_n = w/2$ , so that stresses that are equal and opposite about the  $x = w/2$  sum to zero to give no net force. In the current case of cantilevers bending because of strains generated internally by light, rather than by external imposition of torques, the additional constraint of no net torque leads to a more complex distribution of stresses which gives rise to more than one neutral surface.

The maximum values for both the curvature  $1/R$  and contraction  $K$  are intimately related to the positions of the neutral surfaces. Differentiating eqns (11) and (12) with respect to the cantilever thickness  $w$  and solving between the resulting equations, we obtain the following relationship:

$$\frac{\partial R}{\partial w} = \frac{3R^2}{w} \frac{\partial K}{\partial w}, \quad (18)$$

thus both  $1/R$  and  $K$  are maximised for the same cantilever thickness. Furthermore, returning  $\partial R/\partial w = \partial K/\partial w = 0$  to either of the differentiated equations, one

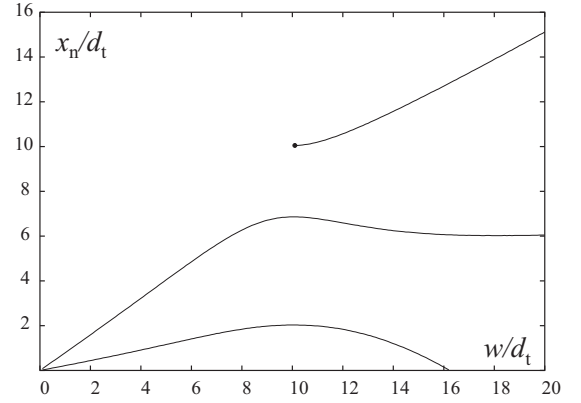


FIG. 10: Neutral surfaces for fixed incident light intensity  $\alpha = 5$  as cantilever thickness  $w$  changes. At the  $w$  maximising curvature, a third neutral surface appears from the rear face; at greater  $w$  a neutral surface is lost at the front face.

finds that the thickness at which this happens,  $w^*$ , satisfies  $w^*/R + K + n_c(w^*) = 0$ , i.e. the straight line of geometrically induced strain intersects the photo-strain ( $\sim n_c(x)$ ) curve at the back surface of the cantilever. The back surface is a neutral surface when the curvature is maximised. The curve  $n_c(x)$  is always a strictly decreasing function of  $x$ ; however there is a fundamental difference between the curves shown in Fig 3 for  $\alpha < 0.5$  and those for  $\alpha > 0.5$  - in the latter case the  $n_c(x)$  curve has a point of inflection ( $n_c''(x) = 0$ ). The straight line of geometrically generated strain imposed from curvature,  $-(x/R + K)$ , can intersect the  $n_c(x)$  curve at most twice if there is no point of inflection, and at most three times if there is a single point of inflection. It is not possible for the strain to satisfy the constraints of vanishing force and torque, that is satisfy eqns (10), and have a neutral surface at the back surface of the beam with only two neutral surfaces; thus there is no maximum for the curvature unless the underlying *cis* curve has an inflection point.

To illustrate the significance of inflections, two sample curvature strains are superimposed in Fig 3. On the  $\alpha = 10$ ,  $\beta = 0$  curve is also plotted the straight line  $-(x/R + K)$  for a cantilever of thickness  $w = 12.5d_t$ , a thickness that is before the inflection point in the  $n_c(x)$  curve. As can be seen, the straight line intersects the underlying  $n_c(x)$  curve only twice in satisfying eqns (10) and locates only two neutral surfaces. On the  $\alpha = 5$ ,  $\beta = 0$  curve is also plotted  $-(x/R + K)$  for thickness  $w = w^* = 10.053d_t$ . One sees that this line intersects the underlying  $n_c(x)$  curve three times, internally twice with the third intersection (neutral surface) coinciding with the back surface. This line is that of maximal possible slope,  $\partial R/\partial w = 0$ . With further increasing thickness,  $d/R$  decreases. Eventually a neutral surface migrates to the front face and is lost. The cantilever continues to have only 2 neutral surfaces thereafter.

Fig. 10 shows how the neutral surfaces change with increasing thickness at fixed illumination  $\alpha = 5$ . With

two regions of compression and two of elongation, one expects subtle behavior when considering compression-induced director rotation[19] in such cantilevers, to which we return elsewhere.

## V. TEMPERATURE EFFECTS

We have neglected the effect of heat generated by absorption of light. Gradients of optical intensity in the cantilever might be expected to generate gradients of temperature and thus of thermal contraction, leading to thermal bend. Experiments where polydomain elastomers bend in the direction of the polarisation of light [11] show directly that optical effects dominate (see the analysis of polydomains in [10])over thermal component of bend. We here quantify the relative size of optical and thermal effects. Let the temperature distribution in the beam be  $\theta(x, t)$ , and take the origin of the temperature scale be such that the ambient temperature outside the cantilever is zero,  $\theta = 0$ . The temperature distribution satisfies a continuity equation in which the heat flux contains the usual thermal gradient term  $-\kappa \frac{\partial \theta}{\partial x} \hat{\mathbf{x}}$  and the divergence of the Poynting flux,  $I(x) \hat{\mathbf{x}}$ , is a source term:

$$C \frac{\partial \theta}{\partial t} - \kappa \frac{\partial^2 \theta}{\partial x^2} = -I_0 \frac{\partial \mathcal{I}}{\partial x} \quad (19)$$

where  $C$  is the specific heat of the the cantilever per unit volume and  $\kappa$  is the thermal conductivity perpendicular to the director, that is along the normal to the flat surface of the cantilever. The diffusion co-efficient  $D$  is given by the ratio  $\kappa/C$ . Typical values for elastomers are around  $\sim 10^{-7} \text{m}^2 \text{s}^{-1}$  [20], with some anisotropy in  $D$  arising in nematic elastomers from anisotropy in the conductivity that we ignore here since thermal effects will in any case turn out to be small. The time taken for heat to diffuse across the thickness of the cantilever is  $\approx w^2/D \sim 0.001 \text{s}$  for a  $10 \mu\text{m}$  sample [11, 21]. For times significantly longer than this, one obtains the steady state solution  $\theta(x)$ . At the front and back surfaces there are convective losses which are described by Newton's law of cooling, that is the heat flux carried away from a surface is  $\delta \theta(0)$  (the temperature outside is  $\theta = 0$ ), where  $\delta$  is the convective heat transfer co-efficient. For free convection in air,  $\delta \approx 5 \text{W m}^{-2} \text{K}^{-1}$ . These convection losses are equal to the thermal flux of heat at the respective surfaces:

$$\begin{aligned} \theta(0) - \frac{\kappa}{\delta} \frac{\partial \theta}{\partial x} \Big|_{x=0} &= 0 \\ \theta(w) + \frac{\kappa}{\delta} \frac{\partial \theta}{\partial x} \Big|_{x=w} &= 0, \end{aligned} \quad (20)$$

where the signs reflect the direction of the outward surface normal. The thermal conductivity is  $\kappa \approx 0.2 \text{W m}^{-1} \text{K}^{-1}$  [22]. The solution to eqn (19) satisfying boundary

conditions is:

$$\begin{aligned} \frac{\theta(x)}{\theta} &= 1 - \frac{\left(1 + \frac{\delta x}{\kappa}\right)}{\left(2 + \frac{\delta w}{\kappa}\right)} \left[1 + \mathcal{I}_w + \frac{\delta w}{\kappa} \int_0^1 \mathcal{I}(wy) dy\right] \\ &+ \frac{\delta w}{\kappa} \int_0^{\frac{x}{w}} \mathcal{I}(wy) dy \end{aligned} \quad (21)$$

The characteristic temperature  $\bar{\theta} = I_0/\delta$  is the temperature that the sample surface would need to attain in order to lose by Newton cooling all the heat equivalent to the incident Poynting energy. Both of the integrals appearing in this expression have been scaled such that their value is bounded by unity. The scale of their contributions is thus set by their pre-factor  $\delta w/\kappa$ . This dimensionless quantity compares the thickness of the sample  $w$  with the thermal penetration length set by the boundary conditions  $\kappa/\delta$ .

There are several interesting limits to this equation:

(i) Using the values for  $\kappa$  and  $\delta$  given above and assuming a cantilever thickness  $w \sim 10 \mu\text{m}$  we obtain  $\frac{\delta w}{\kappa} \approx 2.5 \times 10^{-4} \ll 1$ , and thus the temperature distribution is essentially constant throughout the sample, that is:

$$\frac{\theta(x)}{\theta} = \left(\frac{1 - \mathcal{I}_w}{2}\right) + O(\delta w/\kappa) \quad (22)$$

A constant temperature through the sample leads to contraction along the long axis of the cantilever, but it will not induce bending, since this requires differential contractions. Therefore in this limit, which is close to experimental reality, bending effects in the steady state are due to the optical effects discussed previously, rather than heating.

(ii) Heat is produced proportionately to the rate optical intensity diminishes. If we are in a regime in which intensity decays linearly with depth into the cantilever (such as the  $\alpha = 10$  case in Fig 2 for  $w \leq 10d_t$ ), that is where  $d\mathcal{I}/dx = \text{const.}$ , then heat is generated at the same rate through the cantilever. In the steady state it diffuses to the surfaces, symmetrically if the surfaces are at the same temperature, and hence heat does not contribute at all to the bending. One sees this since now eqn (21) becomes:

$$\frac{\theta(x)}{\theta} = \left(\frac{1 - \mathcal{I}_w}{2}\right) \left[1 + \frac{\delta w}{4\kappa} - \frac{\delta}{\kappa w} \left(x - \frac{w}{2}\right)^2\right], \quad (23)$$

a temperature distribution which is indeed symmetric about the mid-point of the cantilever. Since the thermally-induced strains are also symmetric, they will not produce bending, although once again it will produce an overall contraction. If the cantilever thickness  $w$  is increased beyond the linear interval in Fig 2, then asymmetry in the heat production starts to occur, with less heat generated towards the back face. However, the magnitude of the asymmetry is reduced by diffusion and the thermal contribution to bend sets in only slowly with increasing  $w$ , see (i) above.

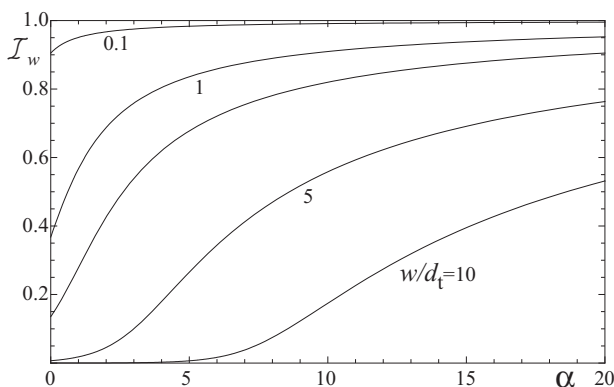


FIG. 11: Scaled intensity at the back surface  $\mathcal{I}_w$  as a function of the incident intensity  $\alpha$  with  $\beta = 0$  for various cantilever thicknesses  $w/d_t$ .

The neglect of heat is thus justified in two limits, firstly the convective heat losses from the boundary are likely to result in a uniform temperature distribution through the sample for the experimentally realistic values of the thermal conductivity  $\kappa$  and the convective heat transfer co-efficient  $\delta$ . Further, in the regime of linear (i.e. non-exponential) decay of intense beams there is no thermal component of bend.

Thermal effects become more extreme, especially in elastomers, if an interior region of the cantilever's temperature exceeds the nematic-isotropic transition temperature. At this temperature an extremely large strain can develop in elastomers, and possibly in glasses. If it occurs in a region symmetrically disposed about the cantilever mid plane, it could lead to pronounced contractions, but not bend. If it occurs in an asymmetrically disposed region, it could lead to large bends – an extreme case we return to in considering specifically elastomers and thus at the same time considering director rotation. Additionally one would there consider the displacement of neutral planes due to volumes of the cantilever suffering large contractions of their natural lengths.

## VI. CONCLUSIONS

We have shown that non-linear absorption (that is, non-exponential profiles) can be invoked to explain how bending can arise in cantilevers where, within Beer's law, one would otherwise expect no response. At high enough incident light intensities, there can be photo-bleaching and thereby penetration of radiation and thus elastic response even in cantilevers so heavily loaded with dye that the Beer penetration depth of the linear regime would be insignificant compared with the cantilever's thickness. The non-linear response in the high dye-loaded limit is possibly of the greatest experimental relevance.

An experiment to explore the non-linear absorption processes we have described would be to measure the intensity at the back surface for a sample of fixed width  $w$  illuminated at the front surface. Altering the incident intensity is equivalent to varying the parameter  $\alpha$ . Scaling the output intensity by its incident value would produce a flat line as a function of  $\alpha$  for simple Beer law attenuation, deviations from a flat line are thus a sign of non-Beer attenuation processes. Figure 11 shows the predicted variation of the reduced exit intensity  $\mathcal{I}_w$  with values of the incident intensity for various cantilever thicknesses in the case  $\beta = 0$ . For thin cantilevers  $w/d_t = 0.1$ ,  $\mathcal{I}_w$  is close to unity, and only increases slowly as  $\alpha$  is increased - for thin cantilevers nearly all of the incident flux is transmitted and there is little absorption. Conversely for thick cantilevers  $w/d_t = 10$  we see that there is very little transmittance for small  $\alpha$ . For larger incident intensities, such that  $\alpha \gtrsim 5$ , the transmittance begins to increase rapidly with  $\alpha$  - a consequence of the increased penetration due to non-linear absorption processes.

Acknowledgement. We are grateful for discussions with David Statman, and to the EPSRC for funding.

- 
- [1] H. Finkelmann and H. Wermter, ACS Abstracts **219**, 189 (2000).
- [2] A. Tajbakhsh and E. Terentjev, Eur. Phys. J. E **6**, 181 (2001).
- [3] H. Finkelmann, E. Nishikawa, G. G. Pereira, and M. Warner, Phys. Rev. Lett. **87**, 015501 (2001).
- [4] J. Cviklinski, A. R. Tajbakhsh, and E. M. Terentjev, Eur. Phys. J. E **9**, 427 (2002).
- [5] G. Mol, K. Harris, C. Bastiaansen, and D. Broer, Adv. Funct. Mat. **15**, 1155 (2005).
- [6] C. van Oosten, C. Bastiaansen, and D. Broer, private communication (2007).
- [7] M. Camacho-Lopez, H. Finkelmann, P. Palffy-Muhoray, and M. Shelley, Nat. Mater. **3**, 307 (2004).
- [8] K. Harris, R. Cuypers, P. Scheibe, C. van Oosten, C. Bastiaansen, J. Lub, and D. Broer, J. Mat. Chem. **15**, 5043 (2005).
- [9] N. Tabiryan, S. Serak, X.-M. Dai, and T. Bunning, Optics Express **13**, 7442 (2005).
- [10] D. Corbett and M. Warner, Phys. Rev. Lett. **96**, 237802 (2006).
- [11] Y. Yu, M. Nakano, and T. Ikeda, Nature **425**, 145 (2003).
- [12] M. Warner and L. Mahadevan, Phys. Rev. Lett. **92**, 134302 (2004).
- [13] M. Kondo, Y. Yu, and T. Ikeda, Angew. Chem. **45**, 1378 (2006).
- [14] D. Statman and I. Janossy, J. Chem. Phys. **118**, 3222 (2003).
- [15] C. Eisenbach, Polymer **21**, 1175 (1980).
- [16] D. Corbett and M. Warner, Phys. Rev. Lett. **99**, 174302

- (2007).
- [17] <http://mathworld.wolfram.com/LambertW-Function.html>.
- [18] M. Abramovitz and I. Stegun, *Handbook of Mathematical Functions* (Dover, New York, 1972).
- [19] R. Verduzco, G. Meng, J. Kornfield, and R. Meyer, Phys. Rev. Lett. **96**, 147802 (2006).
- [20] A. W. Broerman, D. C. Venerus, and J. D. Scheiber, J. Chem. Phys. **111**, 6965 (1999).
- [21] C. L. van Oosten, K. D. Harris, C. W. M. Bastiaansen, and D. J. Broer, Eur. Phys. J. E **23**, 329 (2007).
- [22] Z. Q. Niu, Q. Y. Chen, S. Y. Shao, X. Y. Jia, and W. P. Zhang, J. Micromech. Microeng. **16**, 425 (2006).